Environment Protection Engineering

Vol. 51 2025 No. 2

DOI: 10.37190/epe250202

JIA QU (ORCID: 0009-0008-3605-9270)[1, 2]
XINXIN YU (ORCID: 0009-0000-4436-6520)[1, 2]
SHAOHONG YOU (ORCID: 0000-0001-6417-1683)[1, 3]
XUDONG LAN (ORCID: 0009-0004-9318-3981)[3, 4]

EFFECTS AND MECHANISM OF CONSTRUCTED WETLAND MICROBIAL FUEL CELL (CW-MFC) IN THE TREATMENT OF FRESHWATER FISH AQUACULTURE WASTEWATER

The freshwater aquaculture sector in China is vast and utilizes a considerable volume of water. Wastewater discharge leads to the deterioration of the water environment. Viable treatment strategies need to be implemented immediately to effectively address this contamination. The constructed wetland microbial fuel cell (CW-MFC) technology shows potential in treating wastewater from freshwater aquaculture. Therefore, the study implemented a CW-MFC system to investigate its effectiveness and process in eliminating pollutants like chemical oxygen demand (COD), inorganic nitrogen, and total phosphorus (TP) from wastewater in freshwater fish farming. Results indicated a 7.46% enhancement in COD removal by CW-MFC when contrasted with artificial wetlands (CW). The removal of NH_4^+-N, NO_2^--N, and NO_3^--N increased by 9.08, 3.99, and 6.73%. TP removal increased by 1.31%. The removal capacity of pollutants was significantly higher in CW-MFC than in CW. In addition, the electron transport system activity (ETSA) of CW-MFC was 33.33% higher than that of CW. CW-MFC significantly improves electron utilization efficiency, thereby promoting denitrification and power generation. Higher extracellular polymeric substances (EPS) content and dehydrogenase (DHA) activity in CW-MFC indicated that electron transfer facilitated microbial degradation of COD. These results demonstrate that CW-MFC has significant advantages in treating freshwater fish aquaculture wastewater compared to conventional CW.

---

[1] Guangxi Key Laboratory of Theory and Technology for Environmental Pollution Control, Guilin University of Technology, Guilin, 541006, China, corresponding author, email address: youshaohong@glut.edu.cn

[2] Collaborative Innovation Center for Water Pollution Control and Water Safety in Karst Area, Guilin University of Technology, Guilin, 541004, China.

[3] Guangxi Science & Technology Normal University, Laibin, 546199, China.

[4] Guangxi Key Laboratory of Green Preparation and Application of Inorganic Materials, Laibin, 546199, China.

1. INTRODUCTION

The aquaculture industry in China holds a prominent position globally, with its output consistently ranking first worldwide for numerous years. After decades of development, freshwater aquaculture has transformed low-density and extensive practices into intensive and industrialized operations characterized by substantial inputs, increased stocking density, and enhanced productivity [1]. However, in the process of development, the ecological balance of aquaculture waters and the protection of the water environment are often ignored. The extensive scale of freshwater fish aquaculture leads to a significant volume of feed input, resulting in the presence of unutilized feed residues in the water. The excrement and decomposing carcasses of farmed fish will additionally contribute to the degradation of water quality, leading to organic pollution and eutrophication characterized by excessive nutrient enrichment such as nitrogen and phosphorus. This will harm the health of farmed animals and thus hinder the sustainable and healthy development of freshwater fish farming [2]. Therefore, we urgently need to take effective measures to control the pollution of freshwater fish aquaculture wastewater.

Currently, extensive research has been conducted on the treatment of wastewater from freshwater aquaculture, which can be categorized into physical, chemical, and biological treatment technologies based on their respective mechanisms [3]. Physical treatment technology is mainly to remove solid wastes such as floating matter and flocculation in sewage by physical means, which plays a certain role in optimizing and regulating water quality. Physical treatment technology is simple and widely used, mainly for solid particles and larger organic particles in wastewater, but less effective for the removal of dissolved substances and microorganisms. The physical treatment technology usually can only achieve the primary treatment of wastewater, which still needs subsequent treatment to meet the discharge standards or reuse requirements. Therefore, the physical treatment technology is mostly used for the pretreatment of freshwater fish aquaculture wastewater. The treatment of freshwater fish aquaculture wastewater often uses a combination of physical and chemical methods. However, physical and chemical treatment technology also has some limitations, such as high equipment investment and operating costs, secondary pollution of residual ozone, and other problems. Biological treatment technology mainly creates a favorable environment for water microorganisms in freshwater fish breeding facilities, speeds up the reproduction rate of microorganisms, and enables them to treat organic matter, nitrogen, and phosphorus in water, to achieve water purification [4].

Constructed wetland (CW) is a technology that utilizes the synergistic effects of soil, artificial media, plants, and microorganisms on physical, chemical, and biological processes to treat sewage [5]. Its mechanism includes adsorption, retention, filtration, redox reactions, precipitation, microbial decomposition and transformation, and plant accumulation. It can effectively remove pollutants in water through aerobic and anaerobic respiration of microorganisms, nitrification, denitrification, and other processes.

CW-MFC technology coupling CW with microbial fuel cell (MFC) is a method to obtain bioelectricity in the wastewater treatment Proc. It achieves sewage purification effect through microbial action, which can enhance pollutant removal ability and produce energy [6]. It does not require a continuous external oxygen supply, which reduces treatment costs. Currently, CW-MFC technologies are generally used to treat dye wastewater, heavy metal pollution, antibiotics, and emerging pollutants [7]. However, only a few scholars examined CW-MFC in aquaculture wastewater. Wang et al. [8] coupled an innovative algae-bacteria microbial fuel cell with constructed wetlands to treat fish pond aquaculture wastewater. The removal rates of chemical oxygen demand (COD), total phosphorus (TP), and total nitrogen (TN) increased by 23.84, 21.44 and 15.07%. The CW-MFC system was employed by Liu et al. [9] for the treatment of mariculture wastewater, resulting in a remarkable NO_X^--N removal rate of 97.10%. Although these studies provide valuable insights into the application of CW-MFC in aquaculture wastewater, the specific processes and mechanisms of pollutant removal in freshwater fish aquaculture wastewater still need to be further refined.

CW-MFC was constructed to treat organic matter, inorganic nitrogen, and phosphorus in freshwater fish aquaculture wastewater. In this study, the effect and mechanism of removing contaminants from freshwater fish aquaculture wastewater by CW-MFC were investigated by combining the morphology and structure characterization of fillers, electron transport system activity (ETSA), extracellular polymer substance (EPS) content, and enzyme activity. It aims to provide a reference for the practical application of CW-MFC in freshwater fish aquaculture wastewater treatment.

2. MATERIALS AND METHODS

Construction of the experimental device. The experiment was conducted in the greenhouse of the Ecological Environment Research Center, Yanshan Campus, Guilin University of Technology. CW-MFC and CW devices were constructed with *Canna indica* L. as wetland plants. Figure 1 shows the CW-MFC and CW devices. The cylindrical bodies of CW-MFC and CW are made of UPVC pipes with a diameter of 30 cm and a height of 75 cm. From bottom to top, 20 cm thick zeolite (particle size 8–10 mm), 20 cm thick activated carbon (particle size 2–4 mm), 15 cm thick ceramsite (particle size 10–15 mm), and 10 cm thick activated carbon (particle size 2–4 mm) were successively filled. The device is up-flow with a water inlet at the bottom. The corresponding water outlets of the zeolite layer, anode layer (lower activated carbon layer), ceramsite layer, and cathode layer (upper activated carbon layer) are EFF1, EFF2, EFF3, and EFF4. The activated carbon of the CW-MFC anode and cathode layers was wrapped by a circular stainless steel mesh to enhance electron transfer. The cathode and anode wires of CW-MFC were titanium and copper wires wrapped with epoxy resin, respectively, and the resistance box was connected to form a closed loop.

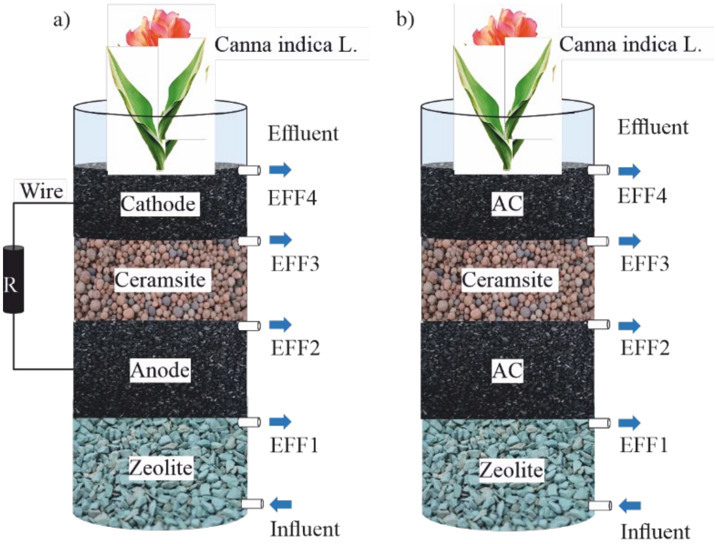

Fig. 1. Schematic diagram of the device for CW-MFC (a) and CW (b)

Startup of the system. Tilapia, yellow catfish, and catfish are widely cultivated freshwater fish species and the concentrations of pollutants in their aquaculture wastewater are at moderate levels. Therefore, according to the concentration of pollutants in the aquaculture wastewater of these three kinds of fish [10], the average value of its indicators was taken to prepare synthetic wastewater to simulate the freshwater fish aquaculture wastewater. The synthetic wastewater consisted of (in mg/dm^3): $C_6H_{12}O_6$ (75.3), NH_4Cl (6.67), KH_2PO_4 (8.3), $NaHCO_3$ (41.6), $MgSO_4$ (3.75), $AlCl_3$ (1.13), H_3BO_3 (0.15), $CaCl_2 \cdot H_2O$ (3.07), $NaNO_2$ (1.86), $CuSO_4$ (4.78). The concentrations of influent pollutants were: COD 81.73–85.91, NH_4^+-N 2.66–2.91, NO_2^--N 1.66–1.75, NO_3^--N 3.84–3.90, TP 1.92–1.98.

The concentrated anaerobic activated sludge used for the experiment was obtained from Yanjing Beer (Guilin Liquan) Co., Ltd. To achieve better acclimatization, the activated sludge was incubated anaerobically for 10 days before being put into the reactor system and afterward inoculated into the reactor. The synthetic wastewater was continuously pumped into the reactor system through a peristaltic pump from the bottom inlet. The start-up was considered complete when a stable biofilm had formed in the device and the effluent's water quality and voltage were stable. After the system reached stability, it was operated for 60 days.

Determination of water quality. Water samples were collected at the outlet of each layer of the system. The influent and effluent water samples were filtered with a 0.45 µm membrane and analyzed within 24 h. COD was determined by the dichromate method (HJ 828-2017). NH_4^+-N, NO_2^--N NO_3^--N, and TP were determined by UV spectrophotometry.

SEM and XRD characterization. Filler samples within the original and post-experiment systems were collected. Scanning electron microscopy (SEM) was used to observe the surface morphology of the samples and the morphology of the electrode biofilm. The acceleration voltage was 3 kV during filming. The phase of each layer of filler was analyzed with an X-ray diffractometer (XRD). It was operated at a voltage of 40 kV and a current of 30 mA. Samples were scanned in a range of $5 < 2\theta < 80$ deg with an interval of 0.02 deg. The results were analyzed using Jade 6.5 software.

ETSA determination. The measurement of electron transport system activity is based on the reduction of iodonitrotetrazolium chloride (INT) by viable organisms in the biofilm sample [11]. First, 2 cm^3 of INT (0.2%) solution was mixed with 1 cm^3 of the sample, and then incubated in a dark room (20 min, 25 °C). 0.2 cm^3 of methanol was added to stop enzyme activity, and centrifuged at 10 000 rpm for 5 min to obtain the precipitate. Next, the insoluble precipitate was resuspended in methanol (4 cm^3, 96%) and mixed thoroughly. The solution absorbance was measured with a spectrophotometer at 495 nm.

$$\mathrm{ETSA}=\frac{A}{15.9}V\times\frac{32}{2}\times\frac{1}{ST}\ \mu\mathrm{g}\ \mathrm{O}_2/(\mathrm{g\cdot min})$$

where A represents absorbance, 15.9 is the molar absorbance, V is the volume of methanol, cm^3, 32/2 is a constant, S is the volume of the sample, cm^3, and T is the reaction time, min.

EPS determination. The anode and cathode samples (40 cm^3) from the CW-MFC system were dehydrated and centrifuged in a 50 cm^3 tube at 6000 rpm for 5 min to obtain a concentrated sample. The sample was diluted to 40 cm^3 with a 0.05% NaCl solution at 70 °C, shaken for 1 min, and then centrifuged at 6000 rpm for 10 min. The supernatant was filtered through a 0.45 μm cellulose acetate membrane to obtain loosely bound EPS (LB-EPS). To obtain tightly bound EPS (TB-EPS), the sample was diluted to 40 cm^3 with a 0.05% NaCl solution at room temperature. The suspension was heated in a water bath at 60 °C for 30 min, then centrifuged at 6000 rpm for 15 min. The supernatant was filtered through a 0.45 μm cellulose acetate membrane to obtain TB-EPS. Finally, the protein (PN) and polysaccharide (PS) contents in the filtrates (TB-EPS and LB-EPS) were measured by the Lowry method and the phenol-sulfuric acid method, respectively.

Enzymatic activity determination. Dehydrogenase (DHA) activity was measured by the TTC (triphenyltetrazolium chloride) colorimetric method. 1 cm^3 of Tris-HCl buffer, a 0.1 mol/dm^3 glucose solution, and a 0.5% TTC solution were added to an Erlenmeyer flask containing 5 g of the sample. It was incubated at 37 °C for 24 h. The reaction was terminated by adding 0.5 cm^3 sulfuric acid. After thorough mixing and adding 5 cm^3 of toluene, the solution was centrifuged at 4000 rpm for 5 min. The organic layer was collected and the solution absorbance at 492 nm was measured. Ammonia monooxygenase (AMO) activity was measured using phosphate buffer at pH 7.4. 20 cm^3 phosphate buffer was added to 5 g of the sample solution, shaken for 30 minutes, then centrifuged. The nitrite content in the supernatant was measured. Nitrate reductase (NR) and nitrite reductase (NIR) activities were measured using assay kits. The activity of alkaline phosphatase (AKP) was measured using the phenyl disodium phosphate colorimetric technique. A mixture of 1 cm^3 toluene and 10 cm^3 phenyl disodium phosphate was added to 5 g of the sample solution. Following a 15-minute agitation, the mixture was maintained at 37 °C for 24 h. After collecting the filtrate, 1 cm^3 was transferred into a flask with a volume of 100 cm^3. Adding 5 cm^3 of borate-sodium hydroxide buffer, 3 cm^3 of potassium ferrocyanide (2.5%), and 3 cm^3 of a 0.5% 4-aminoantipyrine solution, distilled water was utilized to achieve a total of 100 cm^3. Following a 25-minute stabilization period, the absorbance level of the solution was recorded at 570 nm.

Data analysis. Differences between the two systems were assessed by one-way ANOVA analysis with paired-samples T-test using IBM SPSS Statistics 27. Statistical differences, statistically significant differences, and statistically extremely significant differences were accepted at $p < 0.05$, $p < 0.01$, and $p < 0.001$, respectively. The mean and standard deviation of the data were calculated using Origin 2021. And all data figures were plotted by Origin 2021.

3. RESULTS

3.1. REMOVAL OF CONTAMINANTS FROM CW-MFC AND CW

Figure 2 shows the effect of COD removal at different stages in CW-MFC and CW. The COD removal rates of CW-MFC and CW are different. The average COD concentrations in the final effluent of CW-MFC and CW were 4.91 mg/dm^3 and 11.29 mg/dm^3, respectively. The average COD removal rates of CW-MFC and CW were 94.27% and 86.81%, respectively. The COD removal efficiency of CW-MFC was 7.46% higher than that of CW. The COD removal ability of CW-MFC was significantly higher than that of CW ($p < 0.001$).

The removal of inorganic nitrogen by the system includes the removal of NH_4^+-N, NO_2^--N, and NO_3^--N. The inorganic nitrogen removal effect of CW-MFC and CW at each stage is shown in Fig. 3. Both systems had a certain removal effect on various inorganic nitrogen pollutants. Moreover, the removal effect of CW-MFC is significantly different from that of CW. The average removal efficiencies of NH_4^+-N, NO_2^--N, and NO_3^--N by CW-MFC were 93.83, 94.92, and 85.62%, respectively.

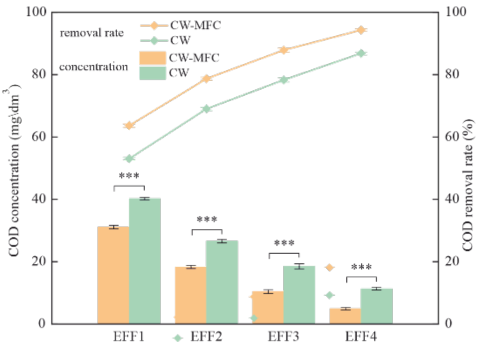

Fig. 2. Effluent COD concentration and removal efficiency at different stages of the two systems; three asterisks (***) indicate statistically extremely significant differences at $p < 0.001$

The average removal efficiency of NH$_4^+$-N, NO$_2^-$-N, and NO$_3^-$-N by CW were 84.75, 90.93, and 78.89%, respectively. The removal efficiencies of CW-MFC were 9.08, 3.99, and 6.73% higher than that of CW, respectively. The removal abilities of NH$_4^+$-N and NO$_2^-$-N by CW-MFC were extremely higher than that by CW ($p < 0.001$), and the removal ability of NO$_3^-$-N by CW-MFC was significantly higher than that by CW ($p < 0.01$).

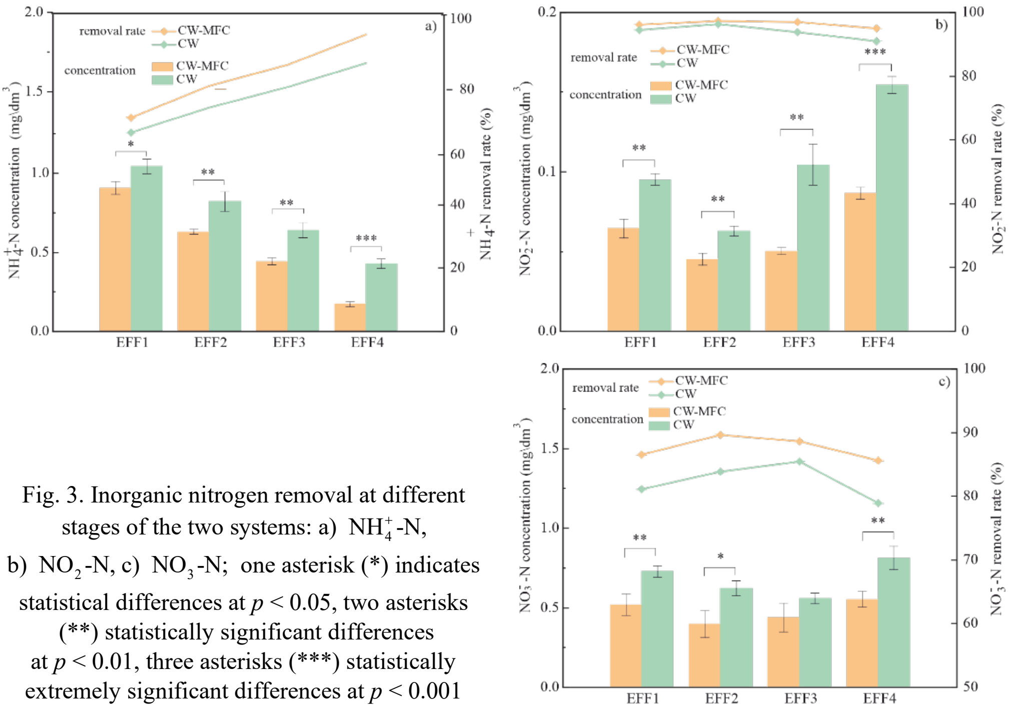

Fig. 3. Inorganic nitrogen removal at different stages of the two systems: a) NH$_4^+$-N, b) NO$_2$-N, c) NO$_3$-N; one asterisk (*) indicates statistical differences at $p < 0.05$, two asterisks (**) statistically significant differences at $p < 0.01$, three asterisks (***) statistically extremely significant differences at $p < 0.001$

Figure 4 shows the removal of TP by CW-MFC and CW. In both systems, the removal of TP showed a gradual increase. The average removal efficiency of TP by zeolite layer in CW-MFC and CW reached about 62.60% and 62.23%, respectively. CW-MFC removed

83.86% TP in the zeolite and anode layers, but only 9.01% TP in the ceramsite and cathode layers. Similarly, CW removed 83.38% of the TP in the first two stages and 8.18% in the last two stages. The TP removal rates of the CW-MFC and CW were 92.87% and 91.56%, respectively. CW-MFC had a higher TP removal ability than CW ($p < 0.05$).

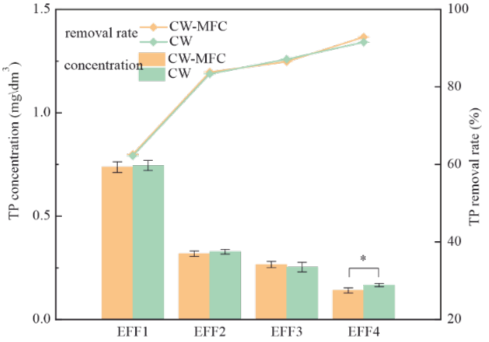

Fig. 4. TP concentration and removal efficiency in effluent at different stages of the two systems; one asterisk (*) indicates statistically significant differences at $p < 0.05$

3.2. CHARACTERIZATION OF CW-MFC FILLERS

Figure 5 illustrates the original surface morphology and structure of the fillers of each layer in the CW-MFC. The surface of zeolite fillers was rough, with protrusions and microporous structures. The surface of the activated carbon filler had porous characteristics and presented a cluster-like structure. The surface of the ceramsite was relatively smooth and had a bulk structure.

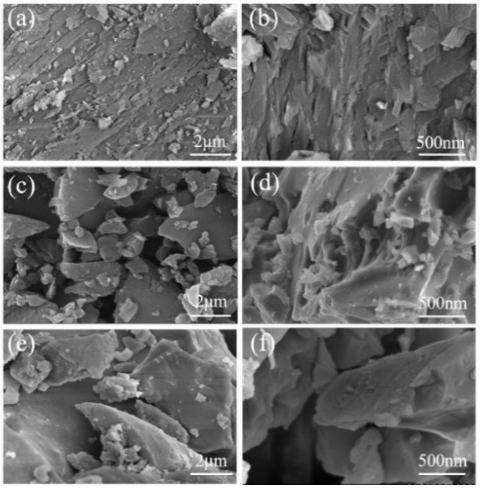

Fig. 5. SEM images of the original fillers of CW-MFC
at two magnifications: a), b) zeolite, c), d) activated carbon, e), f) ceramsite

In Figure 6, the surface structure and form of each layer's fillers post-CW-MFC operation are depicted. A large number of micro nanoparticles accumulated on the surface of the zeolite filler compared to the original filler, and rod-shaped microorganisms were observed. A dense biofilm was formed on the surface of the activated carbon filler. The biofilm on the surface of the ceramsite was thin-layered.

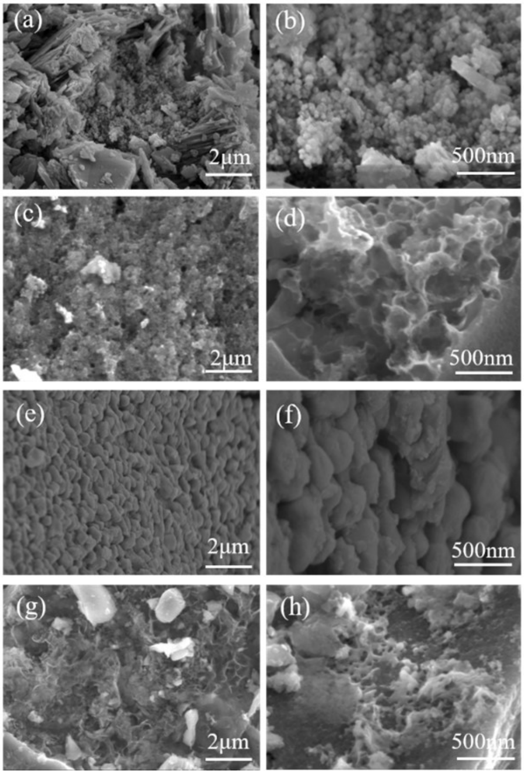

Fig. 6. SEM images of each layer of the filler after CW-MFC operation at two magnifications: a), b) zeolite, c), d) anode-activated carbon, e), f) ceramsite, g), h) cathode-activated carbon

X-ray diffraction (XRD) analysis was conducted on the fillers of each layer to delve deeper into the contaminant elimination process of CW-MFC, both before and following its operation. Figure 7 shows the XRD patterns of the zeolite filler. The main characteristic peaks of both the original zeolite and the zeolite in CW-MFC were mordenite and polyhalite. After the CW-MFC operation, a new diffraction peak of hydrogen phosphate appeared at 29.85°.

Figure 8 shows the XRD patterns of the activated carbon filler before and after CW-MFC operation. Two distinct peaks appeared around the diffraction angles of 23.78°

and 43.4°, corresponding to the (002) and (101) crystal planes of graphite [12]. Both the original activated carbon and the anode/cathode-activated carbon in the CW-MFC system possess typical graphitic structures, with no significant changes in crystal structure. However, the (002) crystal plane of both the anode and cathode shifted from 23.78° to 22.81°.

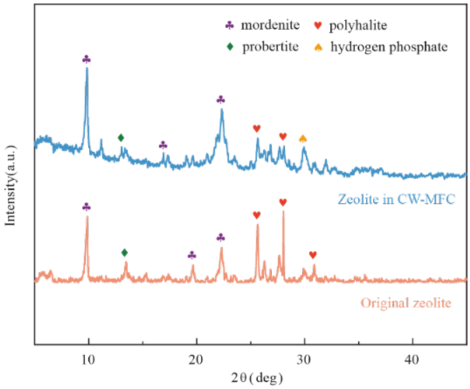

Fig. 7. XRD patterns of zeolite

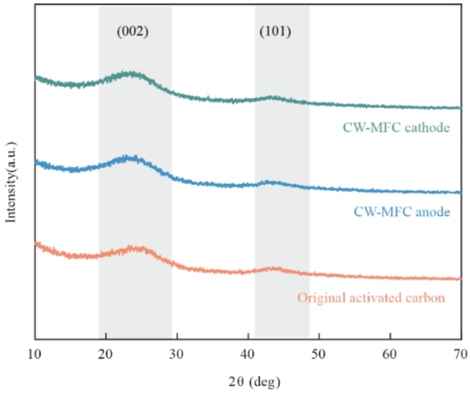

Fig. 8. XRD patterns of activated carbon

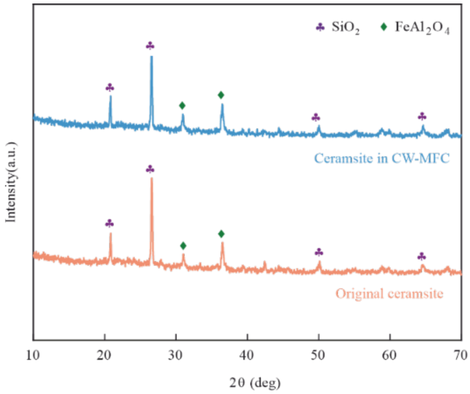

Fig. 9. XRD patterns of ceramsite

Figure 9 shows the XRD patterns of the ceramsite filler before and after CW-MFC operation. The diffraction peaks at 20.81°, 26.56°, 50.12°, and 64.56° correspond to SiO_2. Diffraction peaks located at 30.05° and 36.49° correspond to $FeAl_2O_4$. The crystal structure of the ceramsite remained the same before and after the operation, and the main components were still silica and iron-aluminum spinel [13].

3.3. CHEMICAL AND BIOLOGICAL PROPERTIES

The generation of electrons in CW-MFC results from the decomposition of organic matter by microorganisms. Figure 10 shows ETSA in both systems. ETSA was

0.012 μg O_2/(g·min) in the CW-MFC and 0.008 μg O_2/(g·min) in the CW. ETSA in CW-MFC was extremely significantly higher than that in CW ($p < 0.001$). Compared to CW, the ETSA in CW-MFC is increased by 50%.

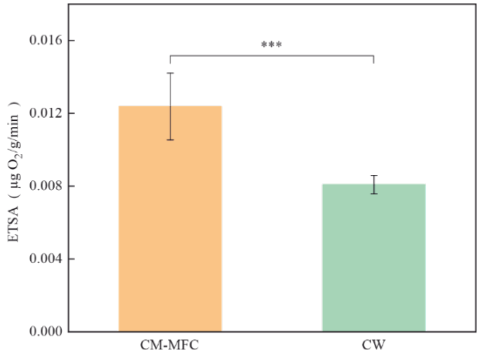

Fig. 10. ETSA in both systems; three asterisks (***) indicate statistically extremely significant differences at $p < 0.001$

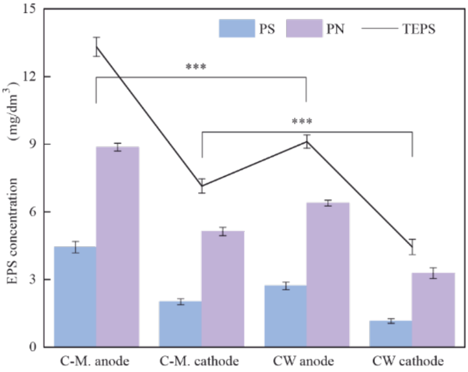

Fig. 11. EPS concentrations in both systems; three asterisks (***) indicate statistically extremely significant differences at $p < 0.001$

Figure 11 shows that the average concentrations of PN and PS at the anode in CW-MFC were 8.87 mg/dm^3 and 4.44 mg/dm^3, respectively. The average concentrations of PN and PS in the cathode were 6.39 mg/dm^3 and 2.72 mg/dm^3, respectively. The sum of PN and PS concentrations represented the total EPS (TEPS). The concentrations of PS and PN in CW-MFC were both extremely significantly higher than those in CW ($p < 0.001$). In both systems, the TEPS contents in the anode region and the lower activated carbon layer (13.31 mg/dm^3 and 7.14 mg/dm^3, respectively) were higher than those in the cathode region and the upper activated carbon layer (9.11 mg/dm^3 and 4.45 mg/dm^3, respectively).

The enzyme activity characteristics of the anode (lower activated carbon layer) and cathode (upper activated carbon layer) in CW-MFC and CW are shown in Fig. 12. The DHA activity at the anode of CW-MFC (45.62 μmol/g/d) was significantly higher than that of CW (39.11 μmol/g/d). The AMO activity of CW-MFC was higher than that of CW, and the AMO activity of the cathode was higher than that of the anode. The NR activity of the anode of CW-MFC (20.23 μmol/g/d) was significantly higher than that of the CW, and the NR activity of the anode was significantly higher than that of the cathode. The NIR activity of the CW-MFC cathode was the highest (69.30 μmol/g/d). The NIR activity was slightly higher at the cathode of the system than at the anode. There was little difference in AKP activity between the two systems. AKP showed low activity compared to the other four enzymes in the system.

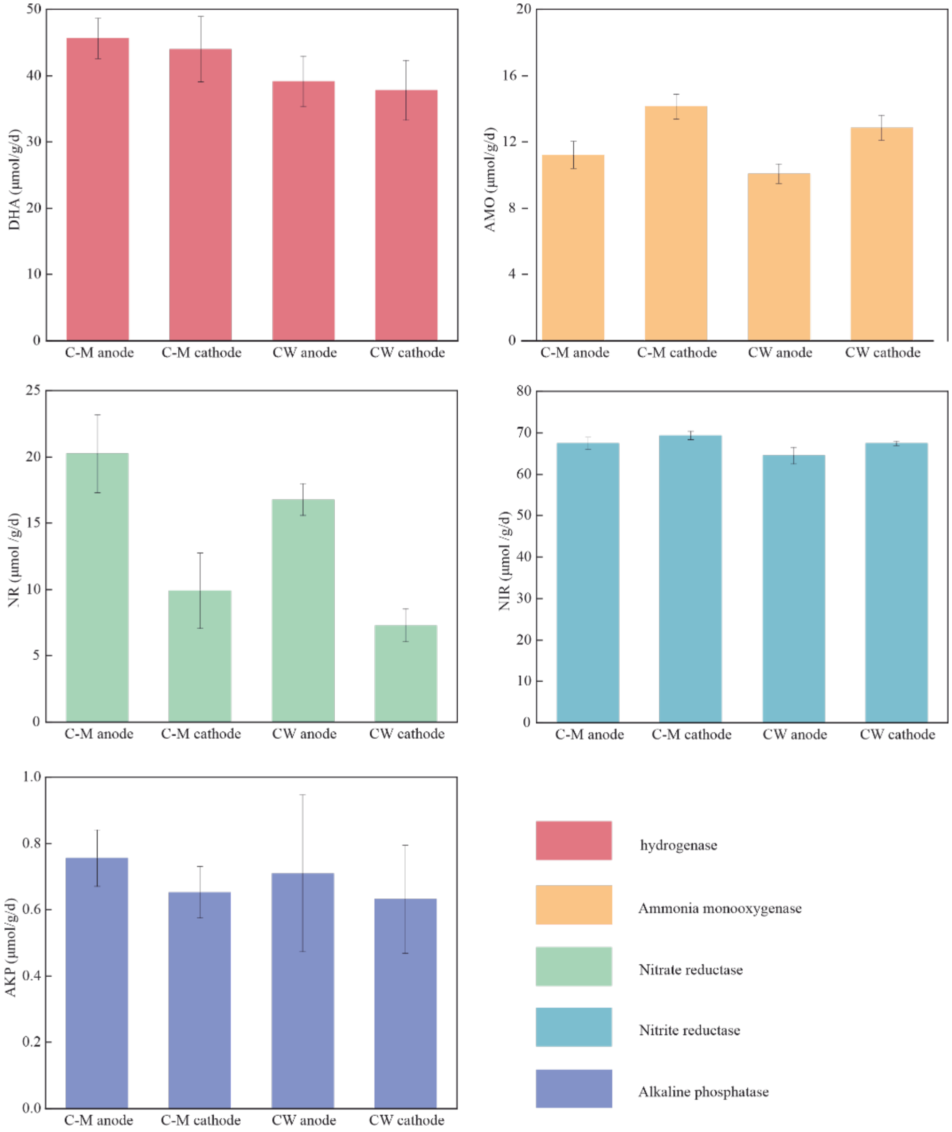

Fig. 12. Activities of five enzymes at the anode and cathode in both systems

4. DISCUSSION

4.1. EFFECT OF CW COUPLED WITH MFC ON CONTAMINANT REMOVAL

The operation mode of CW-MFC can make electrochemical microorganisms have higher abundance and thus higher microbial activity, which is the reason for the high

COD removal rate [14]. Zeolite and ceramsite have good adsorption properties and ion exchange ability, and have developed pore structure and high specific surface area, which provide adhesion points for microorganisms and promote microbial decomposition of organic matter [15]. In addition, zeolites in CW-MFC may have improved their surface conditions due to electric currents, thus increasing microbial activity [16]. In contrast, zeolite and ceramsite in CW can also provide good physical adsorption and microbial growth platforms. However, due to the lack of current promotion, the COD removal rate is relatively low.

Due to the formation of a complete microbial fuel cell pathway in CW-MFC, electrochemical bacteria, and ammonia-oxidizing bacteria have a higher abundance, which can enhance nitrification [17]. This is consistent with the high removal rate of NH_4^+-N by CW-MFC in this study. A study by Teoh et al. [18] showed that NO_3^--N in up-flow CW-MFC wastewater was effectively removed after entering the anaerobic zone at the bottom of the unit, but it increased in the cathode emerging water. In the aerobic region of the cathode, the nitration process produced NO_2^--N and NO_3^--N, and the concentration of NH_4^+-N in the effluent decreased while the concentration of NO_3^--N and NO_2^--N increased correspondingly. In this study, the increase of NO_2^--N and NO_3^--N concentrations of CW-MFC in the ceramsite filler layer was due to the competition generated by the electronic power generation and denitrification processes in CW-MFC. However, NO_2^--N and NO_3^--N in CW could be used as electron acceptors for anaerobic respiration of denitrifying bacteria, and nitrification occurred, thus increasing the removal rate of NO_3^--N in an anaerobic region of CW [19]. When wastewater passes through the CW-MFC cathode region, NH_4^+-N is converted to NO_2^--N and NO_3^--N by nitration. A portion of NO_2^--N and NO_3^--N diffused into the anaerobic region and removed by denitrification ($NO_3^- \rightarrow NO_2^- \rightarrow N_2O \rightarrow N_2$), and the other part was not removed in time. Therefore, the concentration of NO_2^--N and NO_3^--N in the effluent from the cathode aerobic zone of CW-MFC increased. The concentrations of NO_2^--N and NO_3^--N in the final effluent of the two systems increased. This is due to the oxygen release and diffusion of plant roots, as well as the aeration of the effluent section, which inhibits the denitrification of microorganisms [20], resulting in nitrification under aerobic conditions. CW-MFC balanced the nitrification and denitrification processes while increasing the removal rate of NH_4^+-N, reduced the accumulation of NO_2^--N, and improved the removal rate of NO_3^--N by promoting denitrification.

The zeolite layer in CW-MFC and CW had a high TP removal rate, which was mainly due to the high adsorption capacity and porous structure of the zeolite. Zeolite contains metal ions that can precipitate with P and can chemically react with phosphorus ions in water to form an insoluble phosphate precipitate [21]. The activated carbon layer promoted the chemical precipitation of TP mainly through physical adsorption and local environmental changes caused by microbial metabolism in the anode region [22]. The adsorption capacity of ceramsite was weaker than that of zeolite and activated carbon, so the removal effect of the ceramsite layer on TP was less. However, the change of DO and plant absorption in the cathode aerobic zone had little effect on the phosphorus removal efficiency. A previous study found that the main method of CW phosphorus removal is the physical and chemical process of the matrix (including interception, precipitation, filtration, precipitation, absorption, adsorption, ion exchange, and complexation) [23]. In general, there was little difference in the TP removal effect between the two systems. The phosphorus removal processes of CW-MFC and CW were mainly determined by physical adsorption and chemical precipitation in the matrix. Microbial adsorption or transformation in CW-MFC can indirectly increase the TP removal rate, so the TP concentration in CW-MFC was slightly lower than that in CW. The use of more efficient phosphorus adsorption materials in the early stages of the system can improve the phosphorus removal efficiency of the system.

4.2. VARIATION OF FILLERS AFTER CW-MFC OPERATION

Zeolite provided abundant adhesion sites and surface areas for microbial growth and retention of suspended solids. After CW-MFC operation, there were microorganisms attached to the zeolite filler, which contributed to the adsorption and degradation of pollutants. Activated carbon's surface biofilm was involved in breaking down organic material, facilitating nitrification, and extracting nutrients [24]. As an ion exchange material, the cations in the porous structure of zeolite exchanged ions with phosphate groups in wastewater, thus forming hydrogen phosphate to precipitate and adsorb phosphate. In addition, chemical reactions associated with microbial activity also caused hydrogen phosphate to deposit on the zeolite surface, forming hydrogen phosphate. These mechanisms, including ion exchange, adsorption, and microbial deposition, work together to promote phosphorus removal from the system. The porous structure of the activated carbon layer also promoted the fixation and stable growth of microorganisms, providing a large number of attachment points. According to Srivastava et al. [25], graphite particles can promote electrode-dependent anaerobic ammonium oxidation in CW-MFC, maintaining the high TN removal capacity and less biomass, thereby avoiding system clogging during operation. Due to the electron transfer, redox reaction and adsorption process in CW-MFC, the electron density and lattice parameters of the activated carbon electrode material changed. Although the overall crystal structure of activated carbon remained largely unchanged, this change reflected its role in the pollutant treatment process.

Although the specific surface area of ceramsite is small, its microporous structure still provided a certain growth space for microorganisms. The biofilm on the surface of ceramsite consisted of microbial communities adapted to lower nutrient levels. Placed the ceramsite layer in the back half of the system helped reduce the risk of microbial attachment and clogging. Because the ceramsite layer was located in the back half of the system, the concentration of pollutants was lower, and the more difficult to degrade or adsorb substances had less impact on it. Therefore, the main function of ceramsite is to provide a stable physical platform.

4.3. CHEMICAL AND BIOLOGICAL CHARACTERISTICS ANALYSIS

ETSA drove the critical degradation stage of the nitrogen cycle and also determined the efficiency of electricity generation. The ETSA in CW-MFC was significantly higher than that in CW, which indicated that CW-MFC improved the electron transport efficiency. CW-MFC promoted a more active microbial metabolism that continuously supplied the produced electrons to electron acceptors. At the same time, the presence of electrodes changed the local redox conditions, making electron transfer more efficient. The redox-sensitive chemical groups on the surface of activated carbon and their positive effect on the denitrification process improved the electron transport efficiency [26]. Therefore, CW-MFC was more efficient than CW electrons, which facilitated the denitrification process and increased the generation of electrical energy.

EPS is secreted by microorganisms and mainly contains PN, PS, nucleic acid, and other biopolymer compounds, constituting the main components of biofilm. EPS plays an important role in promoting the aggregation of microbial cells, accelerating the rapid formation of biofilm, and removing pollutants. In this study, the PN content of both systems was higher than PS because PN played a dominant role in the formation of biofilm, which reflected the stability and good physiological state of the biofilm of the system [27]. EPS was more abundant in the anode region, which helped control the fluctuation of pollutant concentration and maintained the stability of the system [28]. The superior biological adsorption property of EPS effectively adsorbed suspended particles, organic matter, and some dissolved pollutants in water bodies. Through the interaction of hydrogen bonds, electrostatic action, and van der Waals force, EPS forms a stable bond with pollutants and enables the physical degradation of wastewater [29]. In addition, EPS can also form precipitation with phosphorus and remove pollutants through chemical combinations. CW-MFC produced more TEPS than CW because CW-MFC provided a larger energy source and electrochemical gradient.

Enzymatic activity may mirror alterations in microbes during the process of purifying wastewater. DHA's role in oxidizing organic substances mirrors the rate at which organic matter in wastewater breaks down and its connection to electron generation [30]. DHA activity in CW-MFC was higher than that of CW, indicating that electron transfer promoted the growth of microorganisms that decompose organic matter. AMO catalyzes the conversion of NH_4^+-N to NO_2^--N and is a key enzyme in nitrification. Its activity directly affects the removal efficiency of NH_4^+-N and the oxidation state of nitrogen in the system. The activity of AMO in CW-MFC was higher than that of CW. This was because CW-MFC provided an additional supply of electrons, increasing the efficiency of nitric acid reduction. NR catalyzed the reduction of nitrate to nitrite, which is the primary stage of the denitrification process. This conversion provided an intermediate product for subsequent further removal of nitrite. The slightly higher NIR activity of the cathode was due to fluctuations in oxygen concentration during operation, thus increasing denitrification activity during periods of low oxygen. NIR further reduced

NO_2^--N to NO or N_2. In the system, AMO, NR, and NIR worked together to form a transformation pathway from NH_4^+-N to N_2. Thus, the ammonium nitrogen in the wastewater was effectively removed and more favorable conditions were provided for the reduction of nitrite. There was little difference in AKP activity between the two systems, and the activity was low. This was because most of the phosphorus in both systems was absorbed by the fillers and assimilated by the plants, and most of the phosphorus was removed in the first half of the system. Therefore, in the later stages of the system, the remaining available phosphorus as the substrate of the AKP was relatively limited, limiting the activity of the AKP.

5. CONCLUSION

CW-MFC was constructed to investigate the effect on the treatment of freshwater fish aquaculture wastewater and the mechanism of pollutant removal. Compared with traditional CW, the CW-MFC system had better removal performance of organic matter, inorganic nitrogen, and phosphorus. The mature biofilm, high EPS and DHA activities on the surface of the CW-MFC anode indicated that COD removal is mainly achieved by anaerobic microbial degradation in the anode region. CW-MFC balanced the nitrification and denitrification processes in the system, reduced the accumulation of NO_2^--N, and improved the removal rate of NO_3^--N by promoting denitrification. However, the accumulation of NO_3^--N in the effluent increased slightly. Therefore, the maintenance of an appropriate DO level in the cathode region of the CW-MFC is crucial for efficient denitrification of the system. The removal of TP by CW-MFC was mainly due to the adsorption fixation of fillers and the assimilation of plants. At the same time, CW-MFC improved the concentration of ETSA, EPS, and enzyme activity in the system, so that the wastewater treatment effect was better than CW. Overall, employing CW-MFC for treating freshwater fish aquaculture wastewater demonstrated notable benefits compared to conventional CW methods. However, the pilot-scale application and the stability under different conditions need to be further verified. Further studies on expanding the practical application of CW-MFC in freshwater fish aquaculture wastewater are recommended to improve its feasibility and effectiveness.

ACKNOWLEDGEMENT

This work was funded by the Natural Science Foundation of China [51868010].

REFERENCES

[1] NEWTON R., ZHANG W., XIAN Z., MCADAM B., LITTLE D.C., *Intensification, regulation and diversification: The changing face of inland aquaculture in China*, Ambio, 2021, 50, 1739–1756. DOI: 10.1007/s13280-021-01503-3.

[2] BOYD C.E., D'ABRAMO L.R., GLENCROSS B.D., HUYBEN D.C., JUAREZ L.M., LOCKWOOD G.S., MCNEVIN A.A., TACON A.G.J., TELETCHEA F., TOMASSO J.R., Jr., TUCKER C.S., VALENTI W.C., *Achieving sustainable aquaculture: Historical and current perspectives and future needs and challenges*, J. World Aquacult. Soc., 2020, 51, 578–633. DOI: 10.1111/jwas.12714.

[3] KASHEM A.H.M., DAS P., HAWARI A.H., MEHARIYA S., THAHER M.I., KHAN S., ABDUQUADIR M., AL-JABRI H., *Aquaculture from inland fish cultivation to wastewater treatment: a review*, Rev. Environ. Sci. Bio /Technol., 2023, 22, 969–1008. DOI: 10.1007/s11157-023-09672-1.

[4] PUNGRASMI W., PHINITTHANAPHAK P., POWTONGSOOK S., *Nitrogen removal from a recirculating aquaculture system using a pumice bottom substrate nitrification-denitrification tank*, Ecol. Eng., 2016, 95, 357–363. DOI: 10.1016/j.ecoleng.2016.06.094.

[5] HASSAN I., CHOWDHURY S.R., PRIHARTATO P.K., RAZZAK S.A., *Wastewater Treatment Using Constructed Wetland: Current Trends and Future Potential*, Proc., 2021, 9. DOI: 10.3390/pr9111917.

[6] EBRAHIMI A., SIVAKUMAR M., MCLAUCHLAN C., ANSARI A., VISHWANATHAN A.S., *A critical review of the symbiotic relationship between constructed wetland and microbial fuel cell for enhancing pollutant removal and energy generation*, J. Environ. Chem. Eng., 2021, 9. DOI: 10.1016/j.jece.2020.105011.

[7] GUPTA S., SRIVASTAVA P., PATIL S.A., YADAV A.K., *A comprehensive review on emerging constructed wetland coupled microbial fuel cell technology: Potential applications and challenges*, Biores. Technol., 2021, 320. DOI: 10.1016/j.biortech.2020.124376.

[8] WANG T., LIN Z., KUANG B., NI Z., CHEN X., GUO B., ZHU G., BAI S., *Electroactive algae-bacteria wetlands for the treatment of micro-polluted aquaculture wastewater: Pilot-scale verification*, Biochem. Eng. J., 2022, 184. DOI: 10.1016/j.bej.2022.108471.

[9] LIU F., ZHANG Y., LU T., *Performance and mechanism of constructed wetland-microbial fuel cell systems in treating mariculture wastewater contaminated with antibiotics*, Proc. Saf. Environ. Prot., 2023, 169, 293–303. DOI: 10.1016/j.psep.2022.11.022.

[10] KASHEM A.H.M., DAS P., ABDULQUADIR M., KHAN S., THAHER M.I., ALGHASAL G., HAWARI A.H., AL-JABRI H., *Microalgal bioremediation of brackish aquaculture wastewater*, Sci. Total Environ., 2023, 873. DOI: 10.1016/j.scitotenv.2023.162384.

[11] SATHISHKUMAR K., LI Y., SANGANYADO E., *Electrochemical behavior of biochar and its effects on microbial nitrate reduction: Role of extracellular polymeric substances in extracellular electron transfer*, Chem. Eng. J., 2020, 395. DOI: 10.1016/j.cej.2020.125077.

[12] ANDERSEN H.L., DJUANDHI L., MITTAL U., SHARMA N., *Strategies for the Analysis of Graphite Electrode Function*, Adv. Energy Mater., 2021, 11. DOI: 10.1002/aenm.202102693.

[13] CHEN Y., WANG N., AN S., CAI C., PENG J., XIE M., PENG J., SONG X., *Synthesis of novel hierarchical porous zeolitization ceramsite from industrial waste as efficient adsorbent for separation of ammonia nitrogen*, Sep. Purif. Technol., 2022, 297. DOI: 10.1016/j.seppur.2022.121418.

[14] LU L., XING D., REN Z.J., *Microbial community structure accompanied with electricity production in a constructed wetland plant microbial fuel cell*, Biores. Technol., 2015, 195, 115–121. DOI: 10.1016 /j.biortech.2015.05.098.

[15] HUANG C., YUAN N., HE X., WANG C., *Ceramsite made from drinking water treatment residue for water treatment: A critical review in association with typical ceramsite making*, J. Environ. Manage., 2023, 328. DOI: 10.1016/j.jenvman.2022.117000.

[16] JADHAV H.S., BANDAL H.A., RAMAKRISHNA S., KIM H., *Critical review, recent updates on zeolitic imidazolate framework-67 (ZIF-67) and its derivatives for electrochemical water splitting*, Adv. Mater., 2022, 34. DOI: 10.1002/adma.202107072.

[17] GONZALEZ T., PUIGAGUT J., VIDAL G., *Organic matter removal and nitrogen transformation by a constructed wetland-microbial fuel cell system with simultaneous bioelectricity generation*, Sci. Total Environ., 2021, 753. DOI: 10.1016/j.scitotenv.2020.142075.

[18] TEOH T., ONG S., HO L., WONG Y., OON Y., OON Y., TAN S., THUNG W., *Up-flow constructed wetland – microbial fuel cell: Influence of floating plant, aeration and circuit connection on wastewater treatment performance and bioelectricity generation*, J. Water. Proc. Eng., 2020, 36. DOI: 10.1016/j.jwpe.2020.101371.

[19] JI B., YANG K., ZHU L., JIANG Y., WANG H., ZHOU J., ZHANG H., *Aerobic denitrification: A review of important advances of the last 30 years*, Biotechnol. Bioprocess Eng., 2015, 20, 643–651. DOI: 10.1007/s12257-015-0009-0.

[20] SAZ C., TURE C., TURKER O.C., YAKAR A., *Effect of vegetation type on treatment performance and bioelectric production of constructed wetland modules combined with microbial fuel cell (CW-MFC) treating synthetic wastewater*, Environ. Sci. Pollut. Res., 2018, 25, 8777–8792. DOI: 10.1007/s11356-018-1208-y.

[21] MOKRZYCKI J., FEDYNA M., MARZEC M., PANEK R., SZEREMENT J., MARCINSKA-MAZUR L., JAROSZ R., BAJDA T., FRANUS W., MIERZWA-HERSZTEK M., *The influence of zeolite X ion-exchangeable forms and impregnation with copper nitrate on the adsorption of phosphate ions from aqueous solutions*, J. Water. Proc. Eng., 2022, 50. DOI: 10.1016/j.jwpe.2022.103299.

[22] GUDE V.G., *Wastewater treatment in microbial fuel cells – an overview*, J. Cleaner Prod., 2016, 122, 287–307. DOI: 10.1016/j.jclepro.2016.02.022.

[23] SOUZA A.D.O., BERNARDELLI J.K.B., SILVA L.D.C., PERRETTO F., NAGALLI A., MYMRIN V., PASSIG F.H., DE CARVALHO K.Q., *Plasterboard sheet applied in vertical-flow constructed wetlands: Nutrients removal, microbial diversity, and mechanisms*, J. Water Process Eng., 2023, 53. DOI: 10.1016/j.jwpe.2023.103811.

[24] WANG Y., LI D., SONG X., CAO X., XU Z., HUANG W., WANG Y., WANG Z., SAND W., *Intensifying anoxic ammonium removal by manganese ores and granular active carbon fillings in constructed wetland-microbial fuel cells: Metagenomics reveals functional genes and microbial mechanisms*, Biores. Technol., 2022, 352. DOI: 10.1016/j.biortech.2022.127114.

[25] SRIVASTAVA P., YADAV A.K., GARANIYA V., LEWIS T., ABBASSI R., KHAN S.J., *Electrode dependent anaerobic ammonium oxidation in microbial fuel cell integrated hybrid constructed wetlands: A new process*, Sci. Total Environ., 2020, 698. DOI: 10.1016/j.scitotenv.2019.134248.

[26] WANG Y., SONG X., CAO X., XU Z., HUANG W., WANG Y., GE X., *Integration of manganese ores with activated carbon granules into CW-MFC to trigger anoxic electron transfer and removal of ammonia nitrogen*, J. Cleaner Prod., 2022, 334. DOI: 10.1016/j.jclepro.2021.130202.

[27] HUANG L., JIN Y., ZHOU D., LIU L., HUANG S., ZHAO Y., CHEN Y., *A Review of the Role of Extracellular Polymeric Substances (EPS) in Wastewater Treatment Systems*, Int. J. Env. Res. Pub. Health, 2022, 19. DOI: 10.3390/ijerph191912191.

[28] YU H., *Molecular Insights into Extracellular Polymeric Substances in Activated Sludge*, Environ. Sci. Technol., 2020, 54, 7742–7750. DOI: 10.1021/acs.est.0c00850.

[29] WANG Y., ZHANG X., YU G., YAO Y., LIN H., *Effects of flow pattern, Leersia hexandra, and circuit mode on the Cr(VI) removal capacity, electricity generation performance, and microbial community of constructed wetland-microbial fuel cells*, Fuel, 2023, 338. DOI: 10.1016/j.fuel.2022.127326.

[30] PAN Y., YU S., XIAO Z., MIN Y., TIAN T., ZHENG Y., ZHAO Q., YUAN Z., YU H., *Re-evaluation and modification of dehydrogenase activity tests in assessing microbial activity for wastewater treatment plant operation*, Water Res., 2023, 246. DOI: 10.1016/j.watres.2023.120737.